Distributed natural areas of Earth covers as verification tool of spaceborne SAR radiometric stability

Distributed natural areas of Earth covers as verification tool of spaceborne SAR radiometric stability

A Zakharov, L Zakharova, V Sinilo and E Ivanychev

V.A. Kotelnikov Institute of Radioengineering and Electronics RAS, Fryazino Branch
Vvedensky square, 1, Fryazino, Moscow region, 141190, Russian Federation

aizakhar@ire.rssi.ru

Abstract. The analysis of the long-term stability of the scattering properties of various types of natural covers was carried out using Japanese PALSAR-1 and PALSAR-2 spaceborne synthetic aperture radar observations. High stability of the reflective properties of the extended objects of the Antarctica and South America, comparable with stability of specialized artificial targets, has been revealed. For that reason, distributed targets under discussion may be considered as suitable targets for spaceborne radars intercalibration and monitoring of their stability.

1. Introduction

Scientific instruments calibration is a procedure providing credibility of the estimation of the parameters of radiophysical models describing scattering properties of the sounding covers. Regular technique of synthetic aperture radars (SAR) calibration is external calibration, assuming the deployment of the reference calibration instruments within the imaged area. Typical calibration scenario may be based on a use of passive calibration targets (trihedral corner reflectors, first of all) and active instruments – transponders or active radar calibrators [1, 2]. Typical accuracy of calibration with corner reflectors about 0.15 dB was achieved in TerraSAR-X (X-band) provided the corner leg length was 2 meters [3-6]; in PALSAR-1 project (L-band) it was 0.67 dB for a corner leg length 2-2.5 m, and even 0.17 dB, if its length is 5 meters [7]. Such a calibration targets look like bright point targets on the radar images. The predictability of these targets radar cross-section (RCS) makes them to be indispensable in the procedure of measuring the system transfer coefficient, and their compactness provides possibility to study the details of SAR two-dimensional impulse response function. The deficiency of the instruments mentioned is in the necessity of the targets deployment in specially arranged study area, provision of power supply for transponders as well activities oriented to the equipment preservation during entire cycle of calibration campaign.

In paper [8] various infrastructure objects in different regions of Russia looking like bright point targets were analyzed as candidates for external calibration, but their yearly temporal stability of was worse than 0.5 dB. Seasonal RCS variations are especially noticeable because of an alteration of scattering media scattering properties as a result of freezing/thawing processes. Infrastructure elements located in the regions with permanently positive air temperatures demonstrate significantly higher temporal stability as a point targets. [9]. However, an impossibility of sufficiently accurate estimations of such a scatterers RCS sufficiently reduces their usability. Natural distributed calibration targets may be another alternative to specialized calibration equipment. Amazon rain forest is well-known and de facto reference area for the calibration of spaceborne SAR operating in various frequency bands.

Thanks to permanently high humidity because of almost all the year rainy weather with 2300 mm level of annual precipitations and stable air temperature 27-28° the area is attractive target for SAR calibration and intercalibration. The stability of Amazon forests normalized cross-section (NRCS) in L-band is about 0.2 dB for decades [10].

The goal of this work is a demonstration of the potential of some other distributed natural targets for spaceborne SAR calibration and intercalibration using Japanese L-band PALSAR-1 (2006-2011) and PALSAR-2 (2014 – nowadays) data.

2. Data processing and discussion

There are two geographical areas explicitly different from the Amazon forests in terms of geophysical characteristics, which may be served as supposedly stable distributed scatterers according to our study. The specificity of the areas is also stable though extreme weather and climatic conditions. These are the surfaces of subglacial Lake Vostok in Antarctica and Atacama Desert in South America. Atacama Desert is hot and permanently dry region in Chile, characterized by low (below 1 mm per year) level of annual precipitations and permanently positive and high (19-20℃ in summer and 13-14℃ in winter) air temperature. This highland area is isolated with to mountain belts – Andes on the East and Chilean coastal range on the west. These high mountain belts prevent moisture transport from either the Pacific or the Atlantic Ocean. Almost the only kind of precipitations in Atacama for many years is water condensation from fogs because of fog adherence to the needles or leaves of trees or other objects on mountains or hills slopes. In figure 1, left, PALSAR-1 image frame covering surroundings of Calama city with center coordinates 22.367°S, 68.812°W is presented.

To calculate maps of the distribution of surface scattering properties stability within the SAR frame we processed 12 SAR images acquired during 26.07.2007 - 19.12.2010. Standard PALSAR frame size is ~70×70 km. Level 1.1 FBS SAR data with 4.5 m azimuth and 4.7 m slant range resolution were coregistered, averaged in the 50×50 pixels window and used to calculate NRCS mean and standard deviations within the frame.

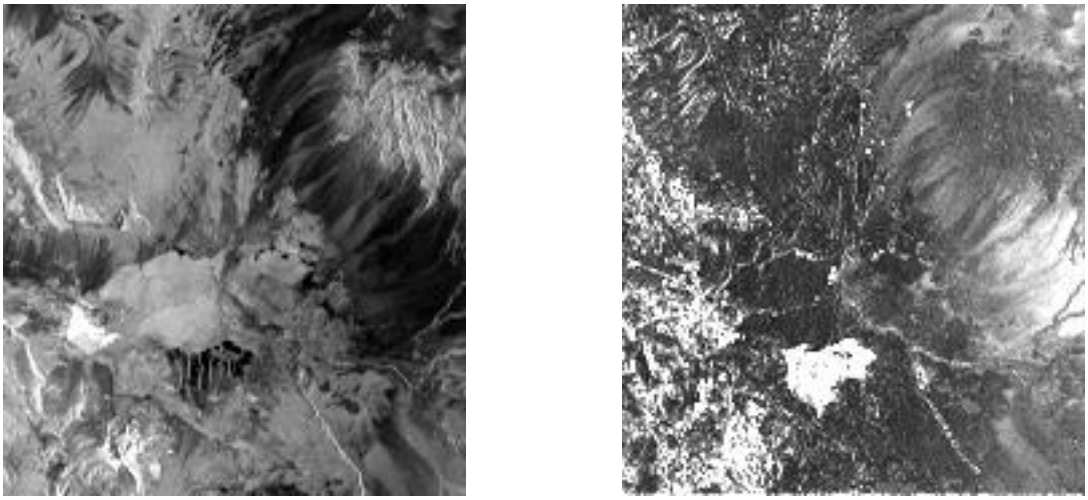

Figure 1. Average Atacama surface NRCS during 4 years (left) and NRCS standard deviation (right) according to PALSAR-1 measurements.

Apparent contrasts on the radar image are typically due to the small-scale roughness, large terrain slopes and variations of the soil dielectric properties. Level of long-term stability of the surface backscatter is presented on the right side of figure 1. Brightness variations here from black to white correspond to stability variations from 0 to 1 dB. Black spot on the stability map to the left from the frame center is rough desert plain area, which is the most stable feature within the frame. The brightest

trapezoidal spot in the image (figure 1, left) — city of Kalama, demonstrating most unstable SAR backscatter level. Bright spots below the center of stability map are settling ponds of the nearby copper ore mines. In general, the left edge of the scene is characterized by increased instability due to vigorous human activity; bright spot on the right edge demonstrates low stability due to the low signal-to-noise ratio on the images of the surfaces with weak backscatter.

Plot of the surface NRCS temporal variations within the 1000×1000 pixels fragment in the upper left corner of PALSAR-1 frame is given in figure 2. Average NRCS here is -15 dB, standard deviation is 0.52 dB.

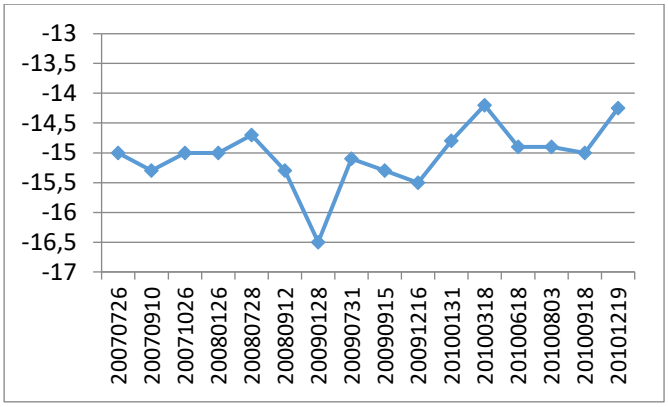

Figure 2. Plot of NRCS temporal variations of PALSAR-1 image fragment during 4 years.

A series of 16 PALSAR-2 images, acquired during 04.10.2014 - 29.08.2020, was used also to compile similar maps of NRCS mean and NRCS standard deviation or stability (see figure 3). Brightness variations from black to white correspond also to the stability variations from 0 to 1 dB. Plot of the surface NRCS temporal variations within the 1000×1000 pixels fragment in the upper left corner of PALSAR-2 frame is give in figure 4. Mean NRCS value here is -17 dB, standard deviation is 0.35 dB. The difference of NRCS mean values is explained by different signal incidence angles and mismatch of the test surface areas within the formally selected averaging window. Within the standard PALSAR-2 frame there are also other relatively small in size areas having outstandingly low NRCS variations, up to 0.19 dB.

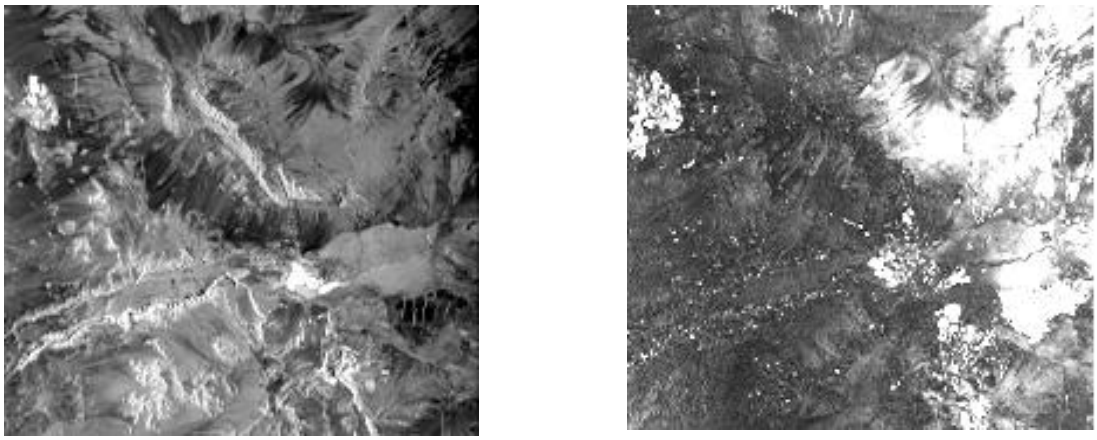

Figure 3. Average Atacama surface NRCS during 6 years (left) and NRCS deviation (right) according to PALSAR-2 measurements.

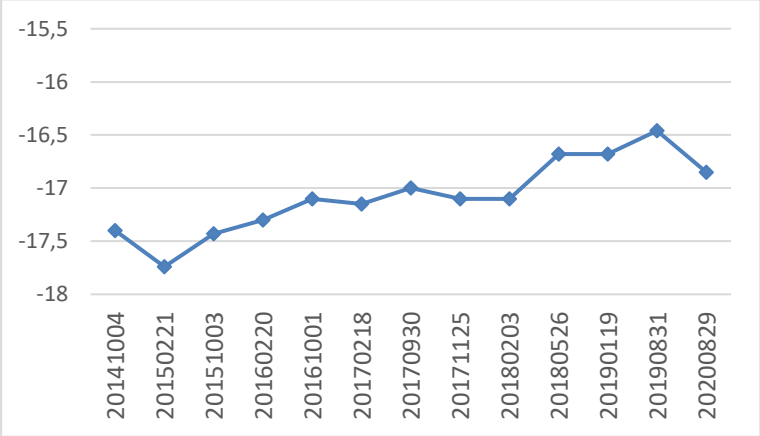

Figure 4. Plot of NRCS temporal variations on PALSAR-2 image fragment during 6 years.

The most attractive surface feature for the purposes of our study, probably, is Lake Vostok located in high latitudes of Antarctica. On the flat surface of the Lake covered with 4 km ice layer there is no any visible manifestation of the bottom topography. Extremal weather conditions with 18 mm annual precipitations and air temperature –65°C in winters and –35°C in summers are common here. Average wind speed in the area is 4-6 m/s with dominating west-east direction (form the left to the right in the image). The snow precipitations from rare snowfalls are blown away by the wind to the east coast, forming snow dunes along the coast (outside this frame). The consequences of snow blizzards on the Lake surface may be seen in a form of short-term 1-2 dB NRCS increase. An example of PALSAR 1 averaged amplitude image with scene center latitude -77.5°S, scene center longitude 105.5°E (frame 5420, path 601) is presented in figure 5. As in the case of Atacama, two maps were calculated using a series of SAR observations during 4 years interval. Left map is a map of mean value of the Lake ice surface NRCS, right one is standard deviation of NRCS. Unlike the Atacama case, brightness variations here from black to white correspond to stability variations from 0 to 0.4 dB. In the lower left corner of the left image in figure 5 one can see hilly coastline of the lake with a thin white line between the hills – the trace of tractor-sledge train connecting Russian high latitudes Antarctic Vostok station with the Progress coastal station. High homogeneity of the surface scattering properties from a point of view of the temporal stability should be underlined: the only apparently unstable feature within the frame in figure 5 is the trace of the tractor-sledge train.

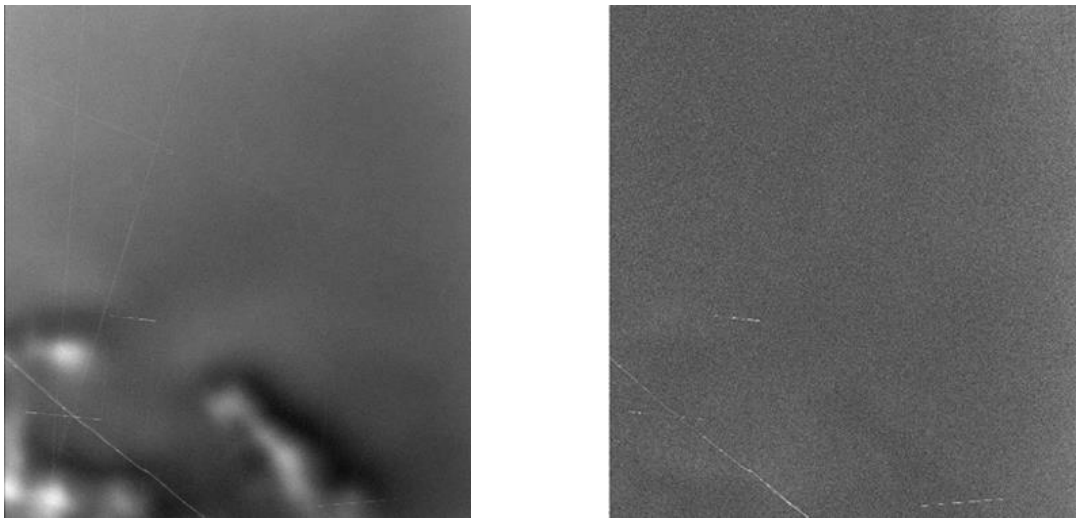

Figure 5. Average Lake Vostok surface NRCS during 4 years (left) and NRCS deviation (right) according to PALSAR-1.

NRCS of the Lake ice covers was averaged in the 500×5000 pixels window of the fragment in the upper left corner of the left image in figure 5. Plot of NRCS variations extracted from 12 PALSAR-1 images is presented in figure 6. Mean NRCS value within the averaging window is –17.8 dB, standard deviation is 0.19 dB.

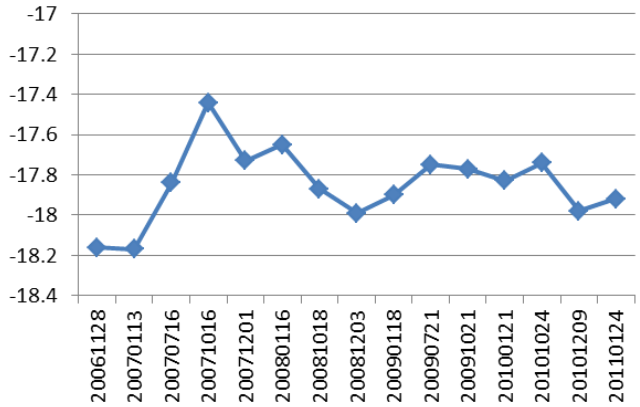

Figure 6. Plot of NRCS temporal variations the Lake Vostok surface fragment according to PALSAR-1 measurements.

Analysis of the same areas with PALSAR-2 data in 2014-2020 conforms high stability of Lake Vostok covers in second decade of our century. The highest stability of the Lake covers backscatter ~0.17 dB for the area in figure 5 was observed in PALSAR-2 data acquired in 2019-2020 from observation path 173. Maps of the RRCS mean value of the Lake Vostok ice surface and standard deviation derived in the processing of PALSAR-2 6 years series of SAR observations look very similar to those in figure 5, and not presented here.

Practically, the only serious drawback of the considered territories in Antarctica may be rather low level of ice sheets NRCS and low radiometric quality of the measurements because of relatively high level of thermal noise. A special unresolved problem of the study area is precipitation in a form of snowfalls, image defocusing on ionospheric irregularities, and Faraday rotation of the signal polarization plane.

3. Conclusion

Natural distributed covers located in Antarctica and South America were explored from a point of view of their backscattering stability. It was discovered that in general their stability is comparable to that of artificial calibration targets like as giant corner reflectors The most stable surfaces, ice covers of Lake Vostok in Antarctica, demonstrate all the year stability of 0.17 дБ during 4-6 years. Provided the conduction of the SAR observations are made in similar observation geometry the distributed natural targets being explored may be recommended as targets for the intercalibration and monitoring of the spaceborne SAR instrument stability.

The work made was conducted according to the State Assignment. Authors appreciate Japanese Aerospace Agency for PALSAR-1 and PALSAR-2 data provided under RA-2 and RA-6 projects.

References

[1] Jackson HD and Woode A 1992 Development of the ERS-1 Active Radar Calibration Unit *IEEE Trans. Geosci. Rem. Sens.* **48**(2) 1063–69
[2] Kenward DRD 1993 A Precision Corner Reflector for ERS-1 SAR Calibration *Can. J. Remote Sensing* 19(3) 218-24
[3] Döring BJ, Schwerdt M and Bauer R TerraSAR-X calibration ground equipment 2007 *Proc. Wave propagation in communication, microwave systems and navigation (Chemnitz, Germany)* (Berlin: VDE Verlag) vol II chapter 4 86-90

[4] Döring BJ, Schrank D, Schwerdt M and Bauer R 2008 Absolute radiometric calibration of TerraSAR-X – approach and ground targets *Microwave Conference* (Berlin: VDE Verlag)
[5] Döring BJ, Reimann J, Raab S, Jirousek M, Rudolf D and Schwerdt M 2014 The three-transponder method: A novel method for accurate transponder RCS calibration *Progress In Electromagnetics Research B* **61** 297–315
[6] Schwerdt M, Bräutigam B, Bachmann M, Döring B, Schrank D and Gonzalez JH 2010 Final TerraSAR-X calibration results based on novel efficient methods *IEEE Trans. Geosci. Rem. Sens.* **40**(6) 677–89
[7] Shimada M, Isoguchi O, Tadono T and Isono K 2009 PALSAR Radiometric and Geometric Calibration *IEEE Trans. Geosci. Rem. Sens.* **47**(12) 3915-32
[8] Zakharov AI, Sorochinsky MV, Zakharova LN and Ivanychev EE 2014 Application of natural point and distributed scatterers for SAR radiometric calibration *Proc. VI All-Russian scientific conference* (Murom) 230-235 https://dropdoc.ru/doc/281827/primenenie-estestvennyh-tochechnyh-i-protyazhennyh-obektov
[9] Yang J, Qiu X, Ding C and Lei B 2018 Identification of Stable Backscattering Features, Suitable for Maintaining Absolute Synthetic Aperture Radar (SAR) Radiometric Calibration of Sentinel-1 *Remote Sens.* **10** 1010
[10] Shimada M 2005 Long-term stability of L-band normalized radar cross section of Amazon rainforest using the JERS-1 SAR *Can. J. Remote Sensing* **31**(1) 132–7